https://scilett-fsg.uitm.edu.my/
Vol. 14(1) JANUARY 2020

ISSN: 1675-7785
eISSN: 2682-8626
DOI: 10.24191/sl.v14i1.10607

The Study of Commercial Titanium Dioxide (TiO_2) Degussa P25 for the Adsorption of Acidic Dye

Nur Shazwani Abdul Mubarak[1,2], S. Sabar[2], Ali H. Jawad[1]*

[1]Faculty of Applied Sciences, Universiti Teknologi MARA, 40450 Shah Alam, Selangor, Malaysia

[2]School of Distance Education, Universiti Sains Malaysia, 11800 Minden, Penang, Malaysia

Corresponding author: ali288@uitm.edu.my

Received: 15 June 2019; Accepted: 1 August 2019; Published: 31 January 2020

ABSTRACT

Commercial titanium dioxide Degussa P25 (TiO_2) was used for the adsorption of reactive red 120 (RR120) dye in a batch system. The optimization functions such as solution pH (3-12), adsorbent dosage (0.02 g-1.2 g), and initial dye concentration (30-400 mg/L) were studied. The equilibrium adsorption data for RR120 dye was analyzed by two types of isotherm models which are Langmuir and Freundlich models. The adsorption at equilibrium showed a better fit for linear Langmuir isotherm with the adsorption capacity, q_{max} of 18.62 mg/g at 303 K. The adsorption kinetic was well-described by pseudo-second order model. TiO_2 showed a decent outcome due to the ability to adsorb target pollutants with the added advantage of providing large hydroxyl groups (OH) on the surface of TiO_2 so that pollutants can be adsorbed by interacting on the surface of OH.

Keywords: *Adsorption; Reactive red 120; Titanium Dioxide; Degussa P25*

https://scilett-fsg.uitm.edu.my/
Vol. 14(1) JANUARY 2020

ISSN: 1675-7785
eISSN: 2682-8626
DOI: 10.24191/sl.v14i1.10607

INTRODUCTION

Titanium dioxide Degussa P25 is commonly known in the field of photocatalytic reaction systems. Degussa P25 is composed of anatase and rutile crystallites typically with a ratio of 70:30 and 80:20. TiO_2 photocatalyst has unique features for widespread environmental applications due to its low price, high photoactivity, high chemical stability, reactivity, and biocompatibility [1]. TiO_2 has excellent sorption characteristics because of the wide surface on the adsorption site [2]. Furthermore, TiO_2 has become one of the most useful substances because many aromatic compounds can be degraded to safe products such as H_2O and CO_2. Other than that, TiO_2 posed an advantage when the pollutants can be adsorbed onto the TiO_2 surface when a high concentration of hydroxyl groups (OH) is present on the surface [3]. Evidence showed that TiO_2 nanoparticles are being discharged into water bodies during their application. The first case of nano-TiO_2 where paints was emitted into urban runoff ruins on building facades. [4]. TiO_2 in the form of nanoparticle is difficult to be removed therefore, increasing the risk of humans and animals being exposed to such pollutant [5].

Photocatalysis is one of the most commonly used techniques for TiO_2 nanoparticles. The abundance of research was found on the photocatalytic reaction in the absorption of dyes from wastewater due to its ability of this technique to completely mineralize the target pollutant [6]. In scientific fact, the adsorption of acidic dye using Degussa P25 is necessary to determine the effectiveness and efficiency of the catalyst. Other than the photocatalysis process, TiO_2 has also been widely used in the adsorption process for the reduction of wastewater pollutants [7]. Fewer findings were reported on the adsorption of TiO_2 because it is widely used in photocatalysis studies and difficult to find any other photocatalyst showing higher activity levels than P25. The benefits of the adsorption process such as convenient, rapid, and inscrutable to toxic contaminants. Herein, we report the adsorption properties of commercial TiO_2 Degussa P25 and the influence of different parameters on the adsorption rate of RR 120 dye.

EXPERIMENTAL

Materials

Titanium dioxide (TiO_2) (Degussa P-25, 80% anatase, 20% rutile) and Reactive red 120 (MW: 1469.34 g/mol; MF: $C_{44}H_{24}Cl_2N_{14}Na_6O_{20}S_6$; λ_{max}: 534 nm) was purchased from Sigma-Aldrich. Acetic acid, hydrochloric acid, and sodium chloride were purchased from R&M Chemicals. Pure water of 18.2 MΩ cm^{-1} was used during this work.

Characterization

pH meter, Metrohm, Model 827 pH Lab, Switzerland was used to determine the value of pH_{pzc}. PerkinElmer, Spectrum RX I in the spectra range between 4000-400 cm^{-1} was used to detect the functional groups of TiO_2 before and after RR 120 adsorption for the analysis of FTIR. Identification of crystalline phases and orientation of the TiO_2 was analyzed by X-Ray diffraction model X'Pert PRO, PAnalytical. Diffraction data are acquired by exposing powder samples to Cu-K_α X-ray radiation.

https://scilett-fsg.uitm.edu.my/
Vol. 14(1) JANUARY 2020

ISSN: 1675-7785
eISSN: 2682-8626
DOI: 10.24191/sl.v14i1.10607

Adsorption experiments

The experiments were done in duplicates to determine the RR120 adsorption capacities. The experimental variables such as adsorbent dosage (0.02 g to 1.2 g), solution pH (3 to 12), initial dye concentration (30 to 400 mg/L), and contact time (0 to 500 minutes) were varied in order to determine the optimum condition. 0.10 M HCl or 0.10 M NaOH were used to adjust the initial pH of RR 120 dye. The samples were placed in an Erlenmeyer flask and agitated in a water bath shaker (Memmert water bath model WNB7-45, Germany) at a fixed shaking speed of 90 strokes/min and 303 K until equilibrium was achieved. The samples then were collected by centrifugation (KUBOTA model 2800) at 2400 rpm for 5 minutes. The solutions obtained were analyzed by using a UV spectrophotometer (model HACH DR2800). The adsorbent uptake, q_e (mg/g), and the percent of color removal, CR% of RR 120 were calculated using equation (1) and (2) respectively.

$$q_e = (C_o - Ce)/Vm \quad (1)$$

$$CR\ \% = (C_o - Ce)/Cox\ 100 \quad (2)$$

where C_o (mg/L) is the initial RR 120 dye concentrations, C_e (mg/L) is the dye uptake at equilibrium, V is the volume of the dye solution (L) and m (g) is the mass of TiO_2.

RESULTS AND DISCUSSION

Characterization of TiO_2 Degussa P25

The pH-dependent surface charges (pH_{pzc}) is solely related to the surface of the particle and the pH of the adsorbate. The analysis was conducted with pH ranging from 2 to 12 as shown in Figure 1. The value obtained for TiO_2 was 6.29 which accounts for the positively charged surface where the pH of the solution was lower than pH_{pzc} [8]. Therefore, RR120 dye is the perfect fit as adsorbate as TiO_2 will bind with negatively charged anions.

https://scilett-fsg.uitm.edu.my/
Vol. 14(1) JANUARY 2020

ISSN: 1675-7785
eISSN: 2682-8626
DOI: 10.24191/sl.v14i1.10607

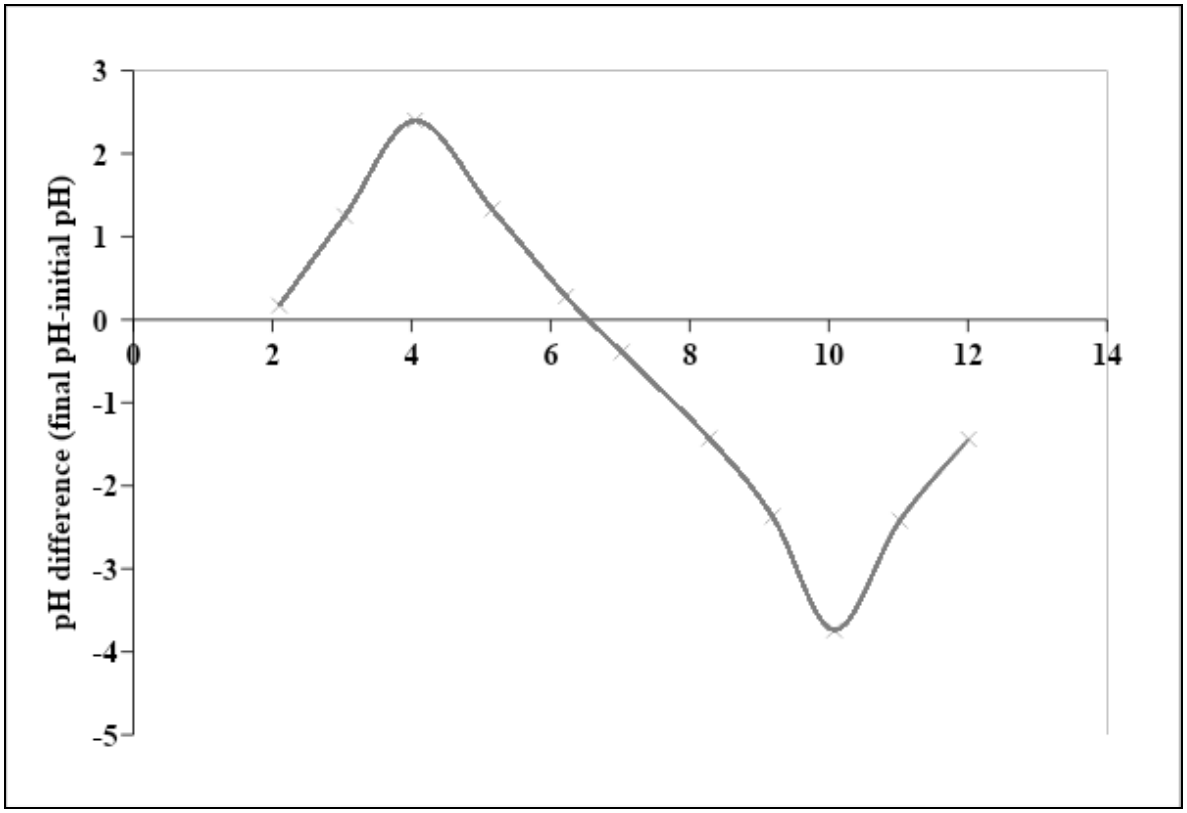

Figure 1: Point of zero charge for all adsorbent. pH_{pzc} for TiO_2: 6.29

https://scilett-fsg.uitm.edu.my/
Vol. 14(1) JANUARY 2020

ISSN: 1675-7785
eISSN: 2682-8626
DOI: 10.24191/sl.v14i1.10607

Spectra of TiO_2 powder before and after the adsorption of RR 120 dye are presented in Figure 2. The noticeable peaks at 1630 and 1625 cm^{-1} are attributed to the deformation mode of molecular water [9]. TiO_2 after adsorption with RR120 dye showed an asymmetric stretching which indicates the presence of sulfonate group (S=O) at 1360 cm^{-1} that is present in the RR120 chemical structure [10].

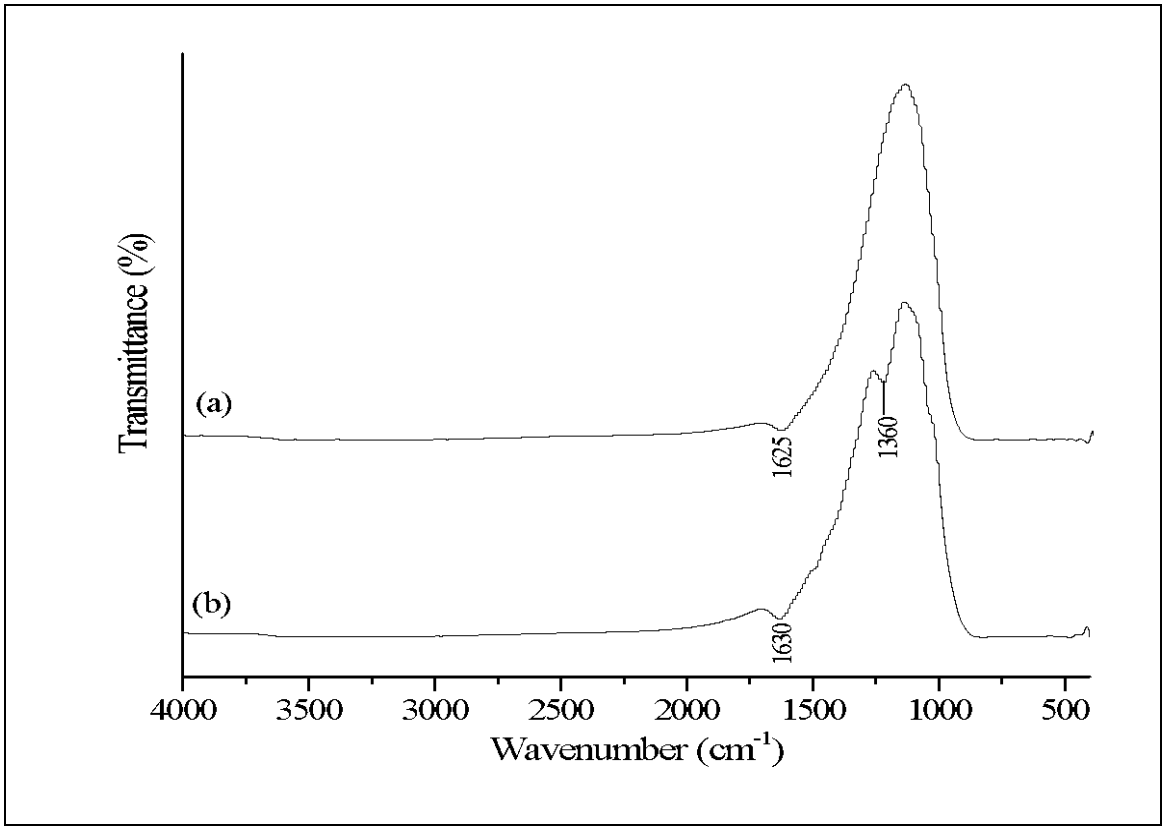

Figure 2: FTIR spectra of (a) TiO_2 before adsorption and (b) TiO_2 after adsorption of RR 120 dye (initial pH = pH 5.22 (unadjusted), $[RR120]_o$ dye = 100 mg/L, volume of solution = 100 mL, shaking speed = 90 strokes/min, T= 303K)

X-Ray Diffraction analysis is an analytical technique for crystalline material that provides phase identification as well as the sample degree of crystallinity. The characteristic diffraction peaks of TiO_2 are presented in Figure 3. The peak at 2θ = 25°, 37°, and 48° correspond to the phase of TiO_2 nanoparticles [11]. According to Ohtani *et al*. [12] the peaks at 2θ = 25° and 27° are isolated anatase and rutile respectively as illustrated in XRD pattern of TiO_2. The strongest peaks depicted at 2θ = 25°, 38°, 48°, 54°, 62°, 68°, 74°, and 82° clearly demonstrated as the anatase phase of TiO_2 nanocrystals [13]. The peak at 2θ = 25° has the highest peak, indicating that the embedding of TiO_2 nanoparticles [11].

https://scilett-fsg.uitm.edu.my/
Vol. 14(1) JANUARY 2020

ISSN: 1675-7785
eISSN: 2682-8626
DOI: 10.24191/sl.v14i1.10607

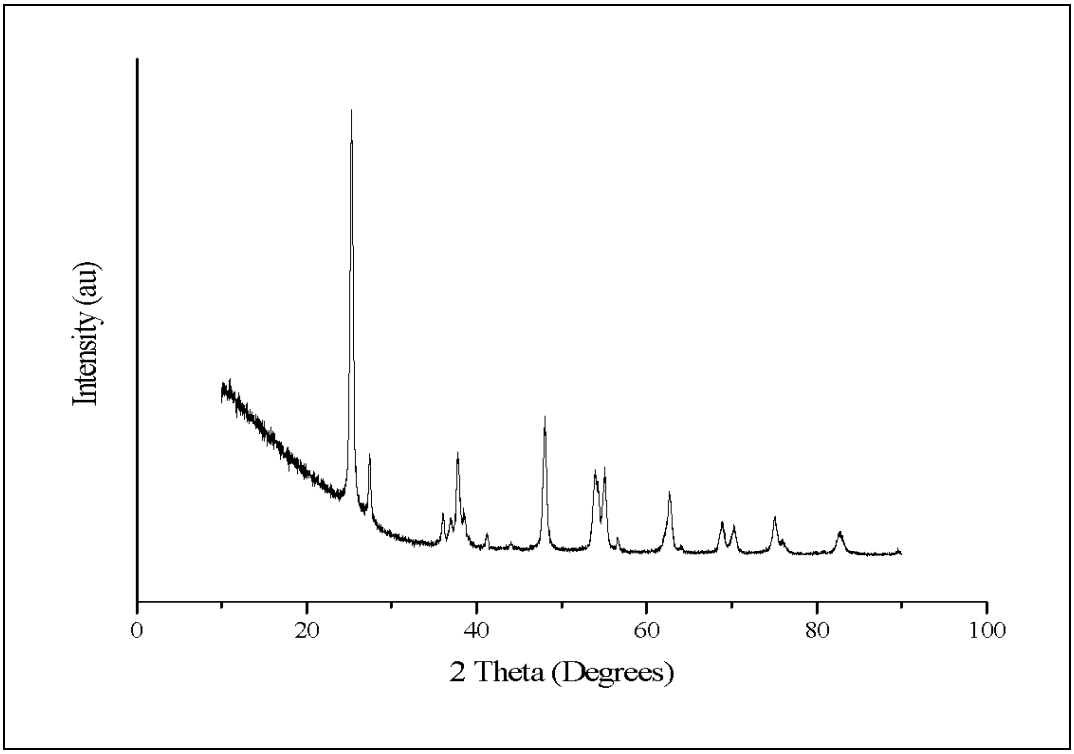

Figure 3: XRD spectrum of TiO_2 Degussa P-25

Adsorption study

Effect of adsorbent dosage

The variables at a concentration of 100 mg/L were analyzed between 0.02 g and 1.2 g. As shown in Figure 4, it is noticeable that the dye removal percentage increase as the amount of adsorbent increase. The percentage of dye removal increase from 15.11% to maximum efficiency of 99.96% where no further progress of dye removal and eventually becomes plateau. The result implies a completed dye removal and no further removal could be achieved even though a large amount of adsorbent were applied [14, 15]. This is due to the mobility of dye ions to the active adsorption sites becomes limited thus reduced the adsorption efficiency [16].

https://scilett-fsg.uitm.edu.my/
Vol. 14(1) JANUARY 2020

ISSN: 1675-7785
eISSN: 2682-8626
DOI: 10.24191/sl.v14i1.10607

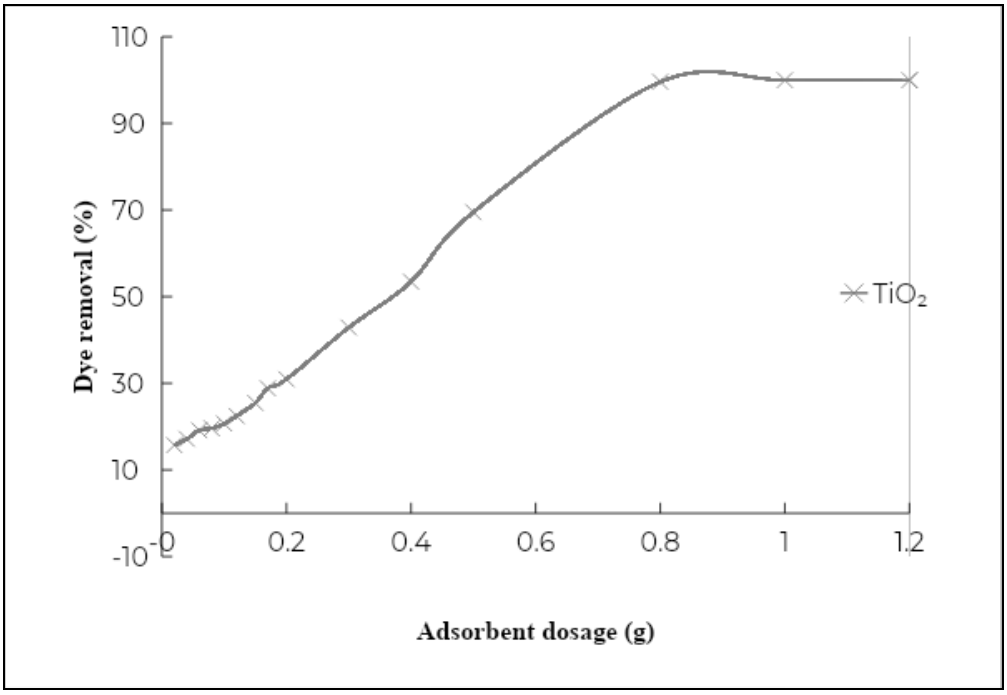

Figure 4: Effect of adsorbent dosage on the percentage removal of RR120 dye. Optimum dosage for TiO_2, is 0.8 g (Initial pH of solution = pH 5.22 (unadjusted), $[RR120]_o$ dye = 100 mg/L, volume of solution = 100 mL, shaking speed = 90 strokes/min and contact time for TiO_2 = 180 min.

Effect of pH

The effect of pH solution contributes significant effects on the degree of ionization and structural changes of dye molecules as well as surface properties of adsorbent [16]. Figure 5 shows the effect of pH on RR120 removal that was accomplished within the pH range of 3-12. The removal of RR120 shows almost the same percentage of removal for pH ranging from 3-9. However, as the pH increases from pH 9-12, the adsorption capacity of RR120 decreases remarkably. At higher pH which is higher than $pH_{pzc,}$ the surface charge becomes negative which will result in the repulsion of dye onto the surface of TiO_2. Conversely, the adsorbent surface acquires a positive charge at lower pH, therefore resulting in an increase of dye adsorption due to increasing electrostatic attraction between positively charged adsorbent and negatively charged adsorbate [17, 18]. The optimum pH used throughout this study is pH 5.

https://scilett-fsg.uitm.edu.my/
Vol. 14(1) JANUARY 2020

ISSN: 1675-7785
eISSN: 2682-8626
DOI: 10.24191/sl.v14i1.10607

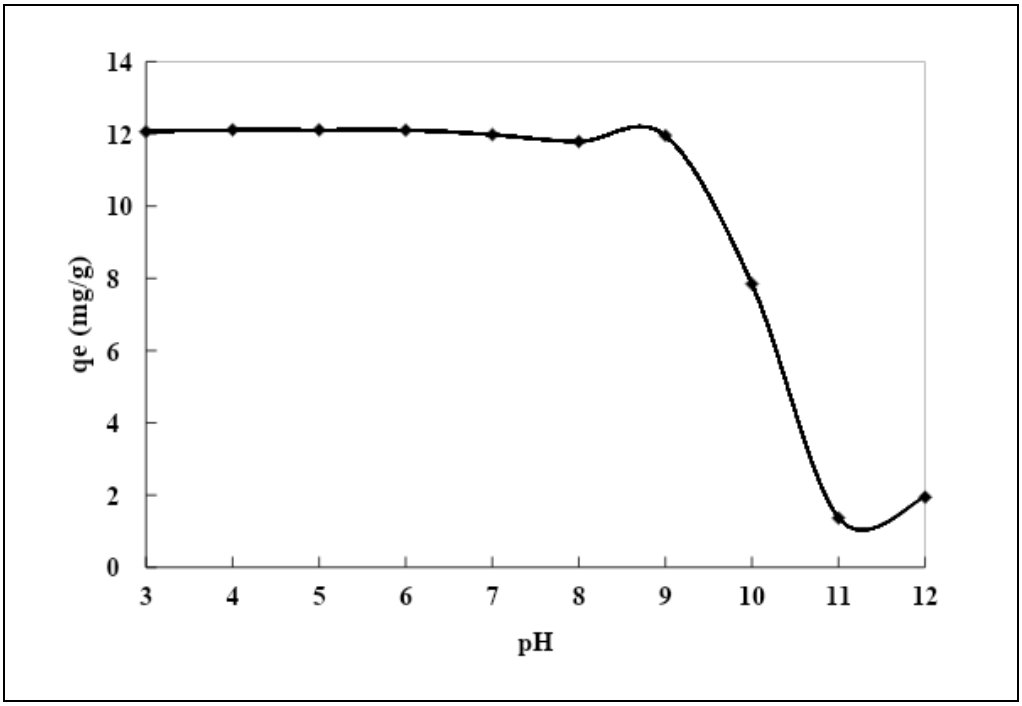

Figure 5: Effect of initial pH on the adsorption of RR120 dyes ([RR120]$_o$ dye = 100 mg/L, amount of adsorbent TiO_2: 0.8 g, temperature: 303 K, contact time: 180 min, agitation speed = 90 strokes/min, and volume of solution = 100 mL)

Initial dye concentration on TiO_2

Figure 6 displays the effect of initial RR120 concentration on the adsorption of TiO_2 at various concentrations ranging from 30 to 400 mg/L. It is noticeable that the adsorption increased tremendously in the first 60 min, after which the adsorption slowed down eventually drawing down to equilibrium at 120 min. The adsorption capacity increased as the initial dye concentration increased from 30 mg/L to 400 mg/L. This phenomenon occurs when the driving force for mass transfer of the concentration gradient increases at a high initial dye concentration [19].

https://scilett-fsg.uitm.edu.my/
Vol. 14(1) JANUARY 2020

ISSN: 1675-7785
eISSN: 2682-8626
DOI: 10.24191/sl.v14i1.10607

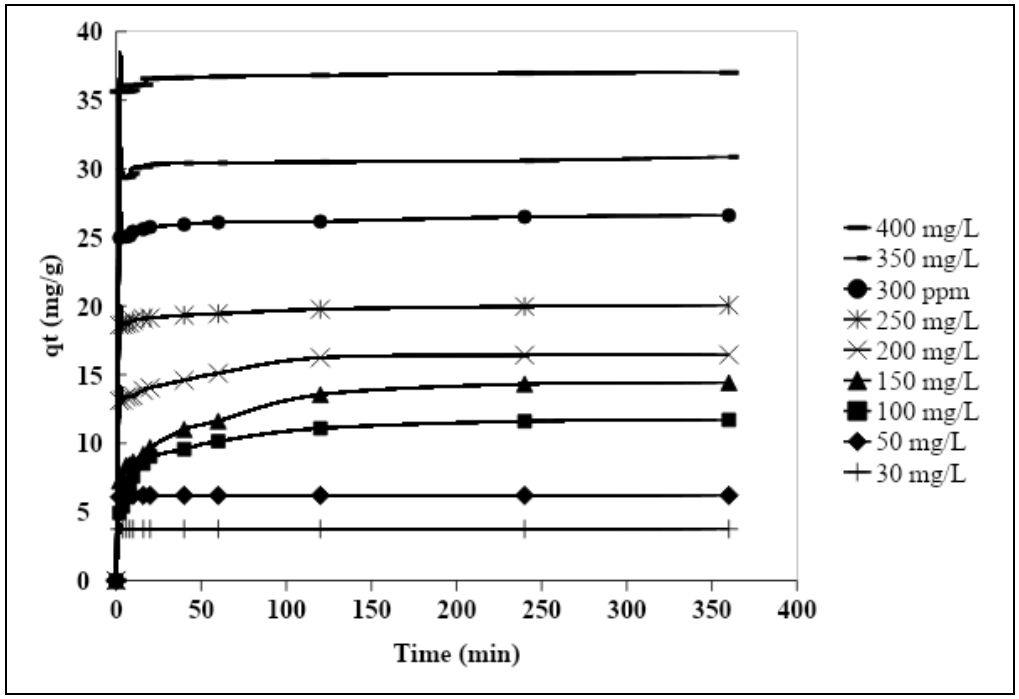

Figure 6: Effect of initial dye concentration on the adsorption of RR120 dye (initial pH of solution = pH 5, amount of TiO_2 adsorbent = 0.8 g, temperature = 303 K, agitation speed = 90 strokes/min and volume of solution = 100 mL)

Adsorption isotherm

Adsorption isotherm commonly defines the behavior of the adsorption process. It describes the molecule distribution of adsorbate between the liquid phase and solid phase once the interaction reached equilibrium. Generally, the adsorption equilibrium can be expressed by various isotherm models. In this study, two commonly used isotherm which is Langmuir and Freundlich models were fitted to determine the most suitable model to represent the adsorption process. The linear form of Langmuir isotherm can be expressed as equation (3)

$$\frac{C_e}{q_e} = \frac{1}{q_m K_L} + \frac{1}{q_m} C_e \qquad (3)$$

where C_e is the equilibrium concentration of TiO_2 adsorbed (mg/L) and q_e is experimental adsorption capacity (mg/g), K_L is the Langmuir equilibrium constant and q_m is the amount of adsorbate required to form a monolayer.

https://scilett-fsg.uitm.edu.my/
Vol. 14(1) JANUARY 2020

ISSN: 1675-7785
eISSN: 2682-8626
DOI: 10.24191/sl.v14i1.10607

Figure 7 shows the plot of C_e/q_e versus C_e where a straight line of a slope ($1/q_m$) and an intercept as ($1/q_m K_L$) is presented.

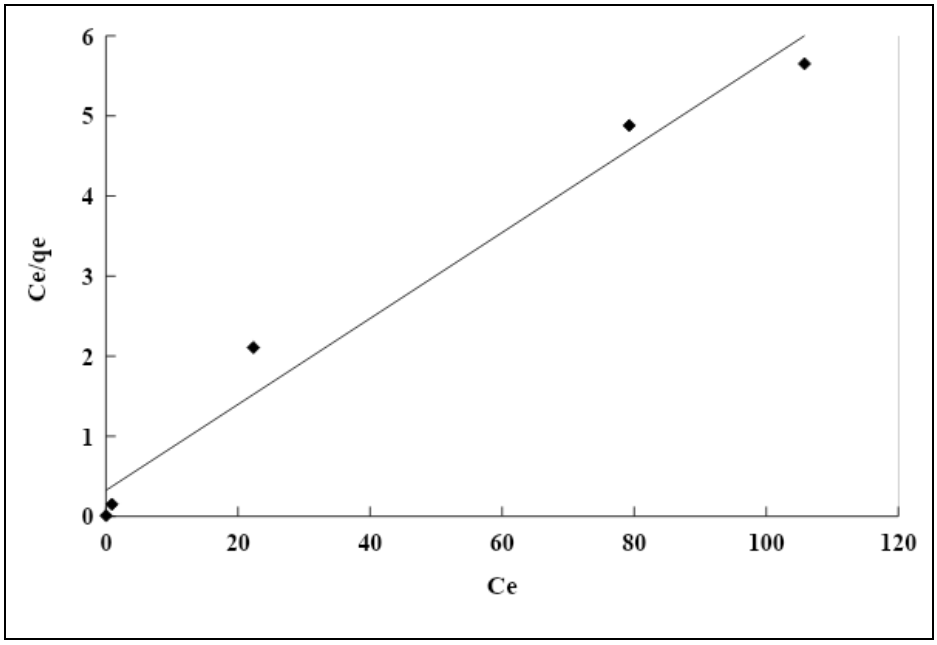

Figure 7: Langmuir isotherm for adsorption of RR120 on TiO_2 (Adsorbent dosage 0.8 g; volume of solution = 100 mL; pH = 5 (unadjusted); T = 303 K)

The Freundlich isotherm is commonly presented as equation (4) [20].

$$\ln q_e = K_f + \frac{1}{n} \ln C_e \qquad (4)$$

where C_e is the equilibrium concentration (mg/L), q_e is the amount of RR 120 adsorbed per unit mass of TiO_2 (mg/g), K_F, and n are Freundlich constants. K_F (mg/g (l/mg) 1/n) gives the information on the adsorption which represents the quantity of dye adsorbed onto adsorbent for a unit equilibrium concentration.

https://scilett-fsg.uitm.edu.my/
Vol. 14(1) JANUARY 2020

ISSN: 1675-7785
eISSN: 2682-8626
DOI: 10.24191/sl.v14i1.10607

Figure 8 shows the plot of ln q_e versus ln C_e.

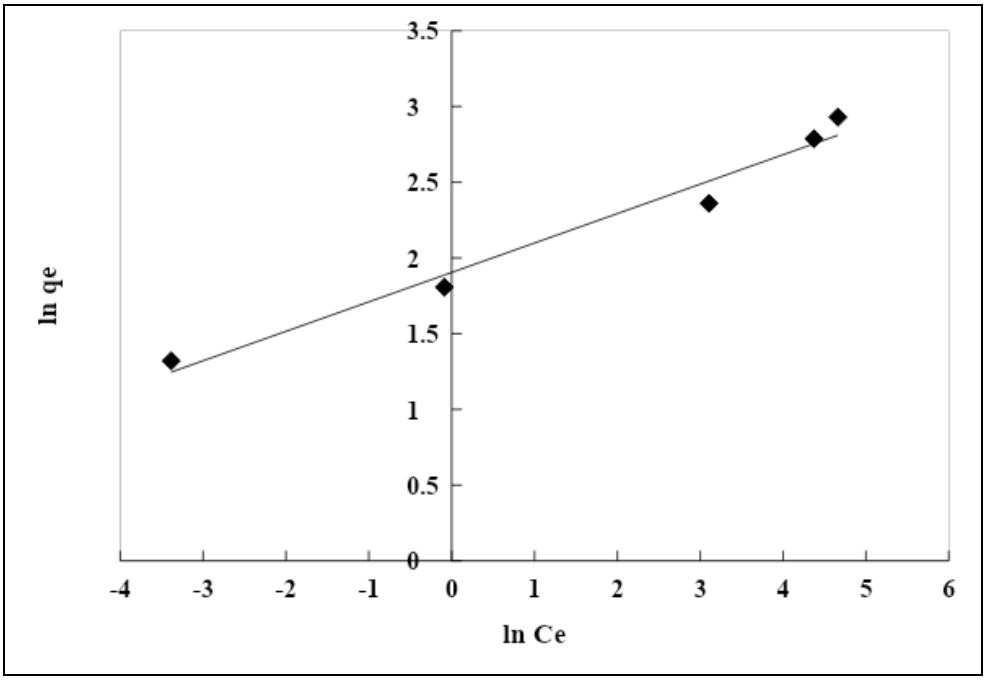

Figure 8: Freundlich isotherm for adsorption of RR120 on TiO_2 (Adsorbent dosage 0.8g; volume of solution = 100 mL; pH = 5; T = 303 K)

As presented in Table 1, the calculation reveals that the adsorption isotherm is best fitted for Langmuir model based on the correlation coefficients. The R^2 value for Langmuir was relatively high as compared to Freundlich models. This proved that the adsorbent has formed a monolayer on the adsorbent surface. The adsorption capacity, q_{max} for TiO_2 was 18.62 mg/g.

Table 1: Isotherm parameters for removal of RR120 onto TiO_2 at 303 K.

Langmuir	**Value**	**Freundlich**	**Value**
q_{max} (mg/g)	18.62	K_F (mg/g (L/mg)$^{1/n}$)	6.71
K_L (L/mg)	0.17	n	5.14
R^2	0.9742	R^2	0.97

https://scilett-fsg.uitm.edu.my/
Vol. 14(1) JANUARY 2020

ISSN: 1675-7785
eISSN: 2682-8626
DOI: 10.24191/sl.v14i1.10607

Adsorption kinetics

The rate-controlling step of the transport mechanism can be determined by interpreting the experimental data obtained, thus pseudo-first-order and pseudo-second-order model were applied [21]. The pseudo first-order model is used to describe the reversibility of equilibrium between liquid and solid phases [22]. The pseudo-first-order rate model was proposed by Lagergren, 1898 [23] and its linearized form can be expressed as equation (5):

$$\ln(q_e - q) = \ln(q_e) - (k_1)t \qquad (5)$$

where q_e (mg/g) and q_t (mg/g) are the amounts of RR120 adsorbed onto TiO_2 at equilibrium and time t, respectively; while k_1 (1/min) is the pseudo-first-order rate constant.

The values of k_1 determined from the slope of the plots of ln ($q_e - q_t$) versus t are presented in Figure 9. The data obtained were summarized in Table 2.

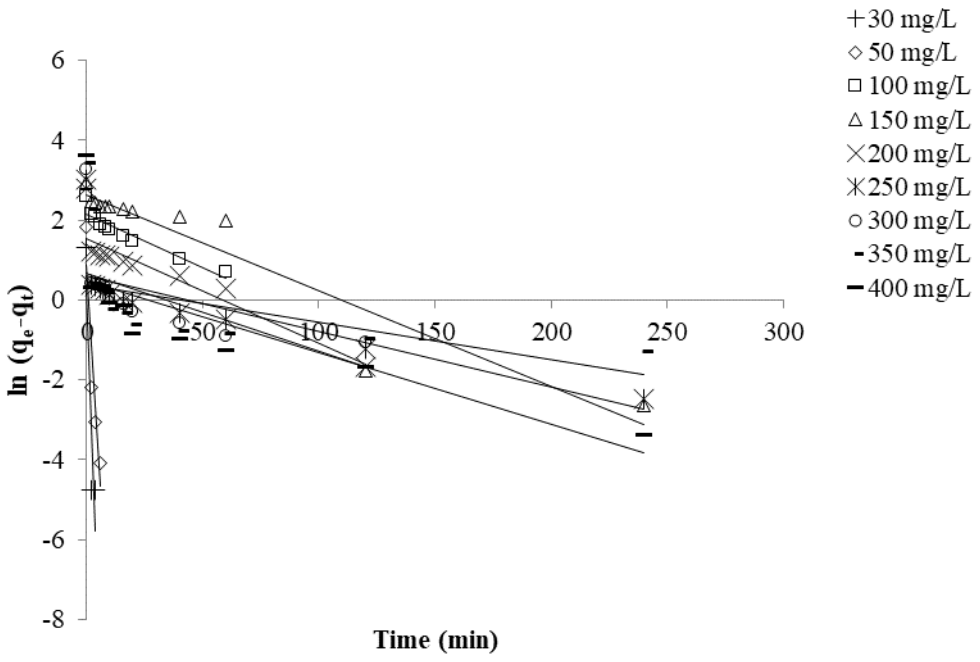

Figure 9: Pseudo-first order kinetics of RR 120 adsorption on TiO_2 at various initial concentrations (adsorbent dosage = 0.8 g; temperature= 303 K; agitation speed = 90 strokes and volume of solution = 100 mL)

https://scilett-fsg.uitm.edu.my/
Vol. 14(1) JANUARY 2020

ISSN: 1675-7785
eISSN: 2682-8626
DOI: 10.24191/sl.v14i1.10607

Table 2: Pseudo first-order kinetic adsorption parameters applied to experimental data for the adsorption of RR120 on TiO_2 at 303 K.

Concentration (mg/L)	**Pseudo- first order**			
	$q_{e,\,cal}$	$q_{e,exp}$	k_1	R^2
30	1.36 ±	3.75	1.5234	0.75
50	2.47 ±	6.09	0.9284	0.85
100	8.62 ±	4.92	0.0270	0.88
150	14.01 ±	7.25	0.0241	0.90
200	4.69 ±	13.09	0.0262	0.81
250	1.81 ±	18.61	0.0139	0.61
300	1.97 ±	24.97	0.0196	0.67
350	1.46 ±	29.36	0.0093	0.88
400	1.63 ±	35.63	0.0179	0.69

The linear form of pseudo second-order equation is generally expressed as equation (6)

$$\frac{t}{q_t} = \frac{1}{k_2 q_e^2} + \frac{t}{q_e} \qquad (6)$$

where k_2 (g/min mg) is the pseudo second order rate constant.

Figure 10 shows the graph of t/q_t versus t, where the values of k_2 and $q_{e\ (Theo)}$, were calculated from the intercept and slope. As displayed in Table 3, the kinetic data for the adsorption of RR120 onto TiO_2 under various conditions was calculated from the related plot and presented in Table 3. The correlation coefficients, R^2 values for pseudo second-order model are much higher than the pseudo first-order model which indicates that the pseudo second order model best describes the adsorption of RR 120 onto TiO_2 powder. The R^2 values were more than 0.99 for all concentrations of RR 120. Moreover, q_e calculated is similar to the q_e experimental for all concentration that was tested. This suggests that the overall rate of the dye adsorption process was controlled by the chemical process and the pseudo second order mechanism was predominant [24].

https://scilett-fsg.uitm.edu.my/
Vol. 14(1) JANUARY 2020

ISSN: 1675-7785
eISSN: 2682-8626
DOI: 10.24191/sl.v14i1.10607

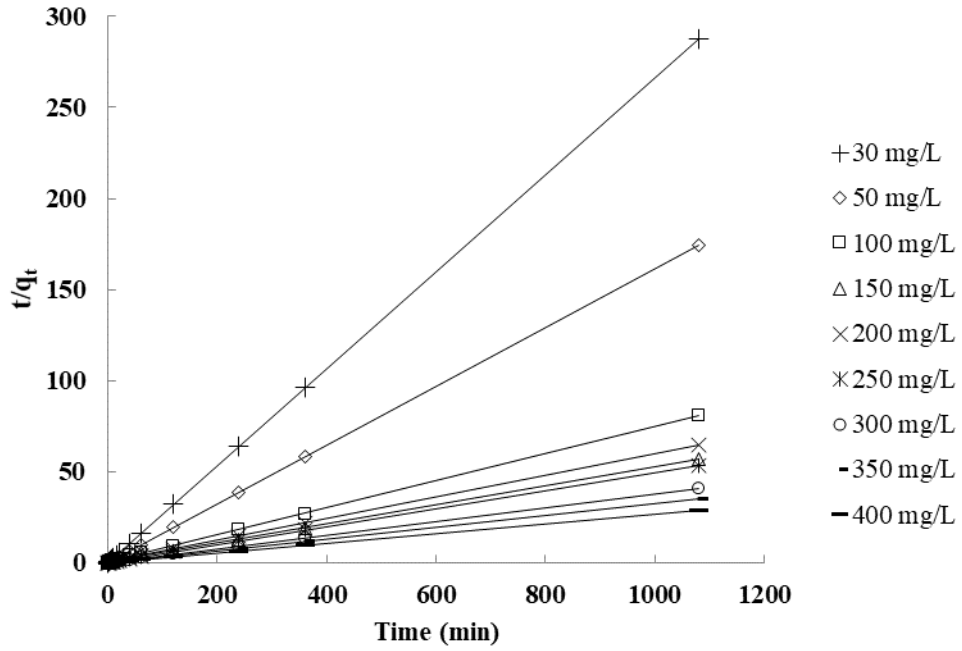

Figure 10: Pseudo-second order kinetics of RR 120 adsorption on TiO_2 at various initial concentrations; adsorbent dosage = 0.8 g; temperature= 303 K, contact time= 180 min; agitation speed = 90 strokes/min and volume of solution = 100 mL)

Table 3: Pseudo second-order kinetic adsorption parameters applied to experimental data for the adsorption of RR120 on TiO_2 at 303 K.

Concentration (mg/L)	**Pseudo-second order**			
	$q_{e,\,cal}$	$q_{e,exp}$	k_2	R^2
30	3.75	3.75	236.56	1
50	6.20	6.20	21.654	1
100	13.50	13.39	0.0122	0.99
150	19.23	18.94	0.0042	0.99
200	16.81	16.79	0.0179	0.99
250	20.37	20.40	0.0285	1
300	26.74	26.75	0.0401	1
350	30.96	30.96	0.0468	1
400	37.45	37.45	0.0291	1

https://scilett-fsg.uitm.edu.my/
Vol. 14(1) JANUARY 2020

ISSN: 1675-7785
eISSN: 2682-8626
DOI: 10.24191/sl.v14i1.10607

CONCLUSIONS

In this work, commercial titanium dioxide TiO_2 was used to conduct the efficiency of adsorption capacity for the removal of dye pollutant RR120 from aqueous solution. Investigation showed that an increase in adsorbent dosage increases dye removal. Moreover, the dye removal increases by decreasing the solution to the acidic environment. The equilibrium data obtained from the experiment can be described by the Langmuir isotherm model whereas the kinetic data are correlated with the pseudo second-order model. The maximum adsorption capacity achieved for the adsorption of RR 120 dye was 18.6 mg/g.

ACKNOWLEDGMENTS

The authors would like to acknowledge Universiti Teknologi MARA for its research facilities and Universiti Sains Malaysia (USM) for the Fellowship granted to Nur Shazwani Abdul Mubarak.

REFERENCES

[1]. Xiao, G., Su, H. & Tan, T., Synthesis of core–shell bioaffinity chitosan–TiO_2 composite and its environmental applications. *Journal of Hazardous Materials*, 283**,** 888-896 (2015).

[2]. Daou, C., Rafqah, S., Najjar, F., Anane, H., Piram, A., Hamade, A., Briche, S. & Wong-Wah-Chung, P., TiO_2 and activated carbon of Argania Spinosa tree nutshells composites for the adsorption photocatalysis removal of pharmaceuticals from aqueous solution. *Journal of Photochemistry and Photobiology A: Chemistry*, 388**,** 112183 (2020).

[3]. Wu, C.-Y., Tu, K.-J., Deng, J.-P., Lo, Y.-S. & Wu, C.-H., Markedly enhanced surface hydroxyl groups of TiO_2 nanoparticles with superior water-dispersibility for photocatalysis. *Materials*, 10**,** 566 (2017).

[4]. Kägi, R., Ulrich, A., Sinnet, B., Vonbank, R., Wichser, A., Zuleeg, S., Simmler, H., Brunner, S., Vonmont, H. & Burkhardt, M., Synthetic TiO_2 nanoparticle emission from exterior facades into the aquatic environment. *Environmental Pollution*, 156**,** 233-239 (2008).

[5]. Liao, G., He, W. & He, Y., Investigation of microstructure and photocatalytic performance of a modified zeolite supported nanocrystal TiO_2 composite. *Catalysts*, 9**,** 502 (2019).

[6]. Yahya, N., Aziz, F., Jamaludin, N., Mutalib, M., Ismail, A., Salleh, W., Jaafar, J., Yusof, N. & Ludin, N., A review of integrated photocatalyst adsorbents for wastewater treatment. *Journal of Environmental Chemical Engineering*, 6**,** 7411-7425 (2018).

[7]. Mubarak, N. S. A., Jawad, A. H. & Nawawi, W., Equilibrium, kinetic and thermodynamic studies of Reactive Red 120 dye adsorption by chitosan beads from aqueous solution. *Energy, Ecology and Environment*, 2**,** 85-93 (2017).

[8]. Ngah, W. W., Teong, L., Toh, R. & Hanafiah, M., Comparative study on adsorption and desorption of Cu (II) ions by three types of chitosan–zeolite composites. *Chemical Engineering Journal*, 223**,** 231-238 (2013).

[9]. Mathew, S., Kumar Prasad, A., Benoy, T., Rakesh, P., Hari, M., Libish, T., Radhakrishnan, P., Nampoori, V. & Vallabhan, C., UV-visible photoluminescence of TiO_2 nanoparticles prepared by hydrothermal method. *Journal of fluorescence*, 22**,** 1563-1569 (2012).

[10]. Pavia, D. L., Lampman, G. M., Kriz, G. S. & Vyvyan, J. A., *Introduction to Spectroscopy*, Cengage Learning (2008).

[11]. Huang, K.-S., Grumezescu, A. M., Chang, C.-Y., Yang, C.-H. & Wang, C.-Y., Immobilization and stabilization of TiO2 Nanoparticles in alkaline-solidificated chitosan spheres without cross-linking agent. *International Journal of Latest Research in Science and Technology*, 3**,** 174-178 (2014).

https://scilett-fsg.uitm.edu.my/
Vol. 14(1) JANUARY 2020

ISSN: 1675-7785
eISSN: 2682-8626
DOI: 10.24191/sl.v14i1.10607

[12]. Ohtani, B., Prieto-Mahaney, O., Li, D. & Abe, R., What is Degussa (Evonik) P25? Crystalline composition analysis, reconstruction from isolated pure particles and photocatalytic activity test. *Journal of Photochemistry and Photobiology A: Chemistry,* 216**,** 179-182 (2010).

[13]. Jani, N.A., pH condition influence nanotube structure of TiO_2 by anodizing titanium substrate. *Science Letters*, **14,** 1-6 (2020).

[14]. Gode, F. & Pehlivan, E., Adsorption of Cr (III) ions by Turkish brown coals. *Fuel Processing Technology,* 86**,** 875-884 (2005).

[15]. Jawad, A. H., Mubarak, N. S. A., Ishak, M. A. M., Ismail, K. & Nawawi, W., Kinetics of photocatalytic decolourization of cationic dye using porous TiO_2 film. *Journal of Taibah University for Science,* 10**,** 352-362 (2016).

[16]. Banerjee, S. & Chattopadhyaya, M., Adsorption characteristics for the removal of a toxic dye, tartrazine from aqueous solutions by a low cost agricultural by-product. *Arabian Journal of Chemistry,* 10**,** S1629-S1638 (2017).

[17]. Shaheed, M. A. & Hussein, F. H., Adsorption of reactive black 5 on synthesized titanium dioxide nanoparticles: Equilibrium isotherm and kinetic studies. *Journal of Nanomaterials,* 2014**,** 3 (2014).

[18]. Jawad, A. H., Mubarak, N. S. A. & Sabar, S., Adsorption and mechanism study for reactive red 120 dye removal by cross-linked chitosan-epichlorohydrin biobeads. *Desalination and Water Treatment,* 164**,** 378-387 (2019).

[19]. Yagub, M. T., Sen, T. K., Afroze, S. & Ang, H. M., Dye and its removal from aqueous solution by adsorption: A review. *Advances in Colloid and Interface Science,* 209**,** 172-184 (2014).

[20]. Freundlich, H., Uber die adsorption in lo sungen. *Z Physics Chemistry,* 57**,** 385-471 (1906).

[21]. Konaganti, V. K., Kota, R., Patil, S. & Madras, G., Adsorption of anionic dyes on chitosan grafted poly (alkyl methacrylate) s. *Chemical Engineering Journal,* 158**,** 393-401 (2010).

[22]. Vijaya, Y., Popuri, S. R., Boddu, V. M. & Krishnaiah, A., Modified chitosan and calcium alginate biopolymer sorbents for removal of nickel (II) through adsorption. *Carbohydrate polymers,* 72**,** 261-271 (2008).

[23]. Lagergren S., Zur theorie der sogenannten adsorption geloster stoffe. Kungliga Svenska Vetenskapsakademiens, Handlingar 24:1-39 (1898).

[24]. Ho, Y.-S. & Mckay, G., Kinetic models for the sorption of dye from aqueous solution by wood. *Process Safety and Environmental Protection,* 76**,** 183-191 (1998).